High Energy Proton Ejection from Hydrocarbon Molecules Driven by Highly Efficient Field Ionization

Stefan Roither,[1] Xinhua Xie,[1] Daniil Kartashov,[1] Li Zhang,[1] Markus Schöffler,[1,3] Huailiang Xu,[2] Atsushi Iwasaki,[2]
Tomoya Okino,[2] Kaoru Yamanouchi,[2] Andrius Baltuska,[1] and Markus Kitzler[1,*]

[1]*Photonics Institute, Vienna University of Technology, A-1040 Vienna, Austria, EU*
[2]*Department of Chemistry, School of Science, The University of Tokyo, Tokyo 113-0033, Japan*
[3]*Lawrence Berkeley National Laboratory, Berkeley, California, USA*
(Received 29 December 2010; published 20 April 2011)

We investigated the ejection of energetic protons from a series of polyatomic hydrocarbon molecules
exposed to 790 nm 27 fs laser pulses. Using multiparticle coincidence imaging we were able to
decompose the observed proton energy spectra into the contributions of individual fragmentation
channels. It is shown that the molecules can completely fragment already at relatively low peak intensities
of a few 10^{14} W/cm^2, and that the protons are ejected in a concerted Coulomb explosion from
unexpectedly high charge states. The observations are in agreement with enhanced ionization taking
place at many C-H bonds in parallel.

Molecular fragmentation is a process of fundamental importance in chemistry and biology. Numerous studies have investigated ionization-triggered fragmentation of multiply ionized molecules created by irradiation with strong, nonresonant laser pulses, e.g., [1–9]. The processes that precede the decomposition of the molecular ion via Coulomb explosion are highly complicated and involve coupled fast electronic [10–12] and slower nuclear motion. Protons take a special role in molecular rearrangement dynamics since they move on a time-scale that is in between the one of the subfemtosecond motion of electrons and the one of the other moieties, which are at least an order of magnitude slower [13–15]. During fragmentation, protons can be ejected with considerable kinetic energy as a result of strong Coulomb repulsion originating either from a large opposing charge, e.g., [5], or a short distance between it and the proton undergoing ejection [16].

We report on the observation of an ionization-fragmentation process that puts a polyatomic molecule into a very high charge state of $+12$ and beyond at laser intensities as low as a few 10^{14} W/cm^2 and subsequently leads to complete molecular decomposition. Our surprising experimental evidence shows that all of the molecule's protons are ejected with high kinetic energies, which is inconsistent with the explanation based on dynamic charge localization used in [16] to explain the proton energy. Furthermore, the energies of all the protons are very similar, which indicates that at the instance of decomposition the protons interact with the same molecular charge state, suggesting an all-at-once (concerted) fragmentation scenario. Therefore, we propose an alternative explanation based on enhanced ionization (EI) [17,18]. We show the mechanism for hydrocarbon molecules using coincidence momentum imaging [19,20], but we believe that such a molecular decomposition process should occur during the

interaction of strong laser pulses with any polyatomic molecule, when the time scale of the intramolecular nuclear motion matches the laser pulse duration. In the particular case of hydrocarbon molecules, the very fast motion of hydrogen atoms in C-H bonds on the order of 10 fs can make this process very efficient even for the interaction with pulses of very short durations down to this time scale.

In our experiments we introduced a supersonic gas jet of either methane, CH_4, ethylene, C_2H_4, 1,3-butadiene, C_4H_6, or hexane, C_6H_{14}, molecules created by expanding the gas samples with a backing pressure of typically $p_b \approx 1$ bar through a nozzle of 10 μm in diameter and subsequent two-stage skimming into an ultrahigh vacuum chamber (background pressure 1.3×10^{-10} mbar). Laser pulses at a repetition rate of 5 kHz with a duration of 27 fs FWHM, centered at a wavelength of 790 nm, were focused by a mirror with a focal length of 60 mm to peak intensities from below 10^{14} up to 10^{16} W/cm^2 onto the molecular jet of ≈ 170 μm in diameter. The created ions were guided by a weak homogeneous electric field of 18 V/cm onto a multihit capable detector equipped with position sensitive delay line anodes. The ion count rate was kept at 0.3–0.4 per laser shot in order to establish coincidence conditions, which ensure that all observed processes take place within a single molecule. In addition this avoids any artifacts connected with high charge density such as space charge effects. We further confirm that the detected ions do not emerge from molecular clusters, that could be created during ultrasonic expansion, by repeating our experiments with a very low backing pressure of $p_r \approx 0.2$ bars for which the probability of clustering is reduced by roughly a factor of $(p_b/p_r)^2 = 25$ [21]. From the measured time of flight and position of each detected ion we calculate its three-dimensional momentum vector in the lab frame.

We obtain background-free kinetic energy spectra of the protons that are created during fragmentations of the four molecules studied by selecting all protons that are emitted towards the detector within a 90° cone. Figs. 1(a)–1(d) show the resulting proton energy spectra for methane (a), ethylene (b), 1,3-butadiene (c) and hexane (d) for linear laser polarization and various peak intensities, which were calibrated with an estimated precision of ±10% by comparison to the highly intensity-sensitive proton energy spectra of molecular hydrogen [22]. While the low energy structures are created by fragmentations of molecular ions from low charge states at smaller laser intensities within the spatial pulse profile, it can be seen that the cutoffs of the proton energy spectra increase monotonically with laser peak intensity and also with the size of the molecules.

Figures 1(e)–1(h) show the cutoff position as a function of laser peak intensity for linear (red) and circular (blue) laser polarization state. First we focus on the data taken with linearly polarized light. Similar proton energy spectra as those in Fig. 1 with analogous cutoff intensity dependence have been measured [16] in the laser induced Coulomb explosion of a much larger polyatomic molecule, anthracene, $C_{14}H_{10}$. For a given molecular geometry the measured fragment kinetic energies are determined by the charge state distribution within the molecule prior to the Coulomb explosion. Based on an estimated charge state a nonadiabatic charge localization was proposed as their origin.

In order to determine the charge states that are connected with the energetic protons that make up the spectra shown in Fig. 1, we performed a multicoincidence selection of our data without restrictions on the ejection direction. By gating on the most energetic protons we find that they are created during fragmentations that result in decomposition of the molecular skeletal structure and the production of bare carbon ions. The carbon ions fulfill momentum conservation such that we can select certain carbon ion fragmentation channels. Because the efficiency to detect n particles in coincidence scales as P^n, where P is the probability to detect one particle which is typically on the order of 0.5, we restrict our analysis to ethylene and 1,3-butadiene. In our coincidence analysis we select the following carbon ion fragmentation channels: C^{m+}-C^{n+}, with m, $n \leq 3$, for ethylene and C^{j+}-C^{k+}-C^{m+}-C^{n+}, with j, k, m, $n \leq 2$, for 1,3-butadiene. For each of these channels we try to find all the protons that are correlated with the carbons. Despite the unfavorable scaling of the detection efficiency, for the ethylene data we manage to select all six ionic fragments that fulfill momentum conservation with an uncertainty of ≈ 4 a.u. FWHM for a few intensity points and a small number of events. In general, however, we restrict ourselves to the selection of 2 (ethylene) or 3 (1,3-butadiene) protons in coincidence with the 2 and 4 carbon ions of ethylene and 1,3-butadiene, respectively. We require that the protons are ejected into the same direction towards the shortest flight times such that we can detect them free of background from slower ion species. It turns out that all protons exhibit identical energy distributions, see inset of Fig. 2(a), where we show the energy spectra of all 4 protons ejected from ethylene for the channel C^+-C^+ as an example. Because the carbon ions fulfill momentum conservation, the high momentum sum of the selected protons needs to be balanced by the same number of protons ejected into the opposite direction. As a consequence our analysis reveals that the most energetic protons are created by a process where the breakage of the molecular carbon skeletal structure is preceded by ejection of all the hydrogen atoms as protons with nearly identical energy.

We show the results of the described channel decomposition for ethylene and 1,3-butadiene in Fig. 2. The colored lines represent the proton spectra that are created
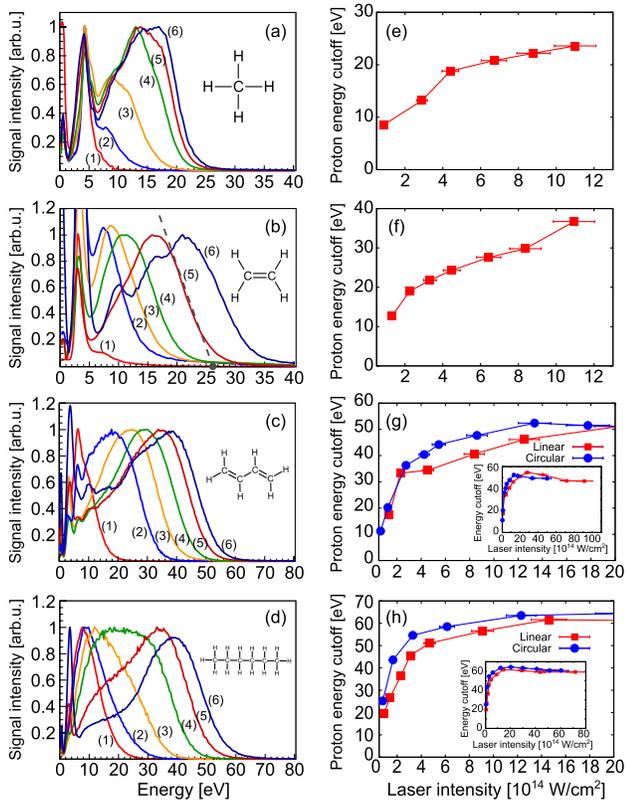

FIG. 1 (color online).   Measured proton energy spectra (a)–(d) and cutoff energies (e)–(h) for methane (a),(e), ethylene (b),(f), 1,3-butadiene (c),(g) and hexane (d),(h) recorded with linearly polarized laser pulses of different peak intensities. The cutoff energy is defined where a tangent on the high-energy part of the spectra cuts the abscissa, as illustrated in (b). The spectra in (a)–(d) from (1) to (6) are shown for the following intensities (in units of 10^{14} W/cm^2): 0.9, 2.9, 4.4, 6.7, 8.8, 11.0 (a); 1.3, 2.3, 3.3, 4.5, 8.4, 10.9 (b); 1.4, 2.2, 4.6, 8.4, 13.5, 18.8 (c); 0.9, 1.4, 2.3, 3.1, 4.7, 9.1 (d). The red squares and blue circles in (e)–(h) correspond to linearly and circularly polarized light, respectively, with the peak intensity defined as the square of the peak field strength in both cases. The insets in (g) and (h) show the saturation of the proton energy cutoff for higher laser intensities.
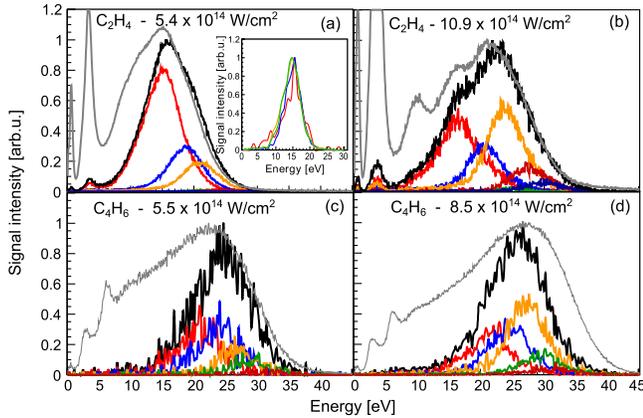
FIG. 2 (color online). Decomposition of the total proton energy spectra (gray lines) taken from Fig. 1 for ethylene (a,b) and 1,3-butadiene (c,d) and pulse peak intensities (in units of 10^{14} W/cm^2) 5.4 (a), 10.9 (b), 5.5 (c), 8.5 (d) into the proton spectra of separate fragmentation channels (colored lines). The black line shows the sum of all individual spectra. Each of the channels consists of 1 proton correlated with 2 carbon ions C^{m+}-C^{n+} for ethylene (6 channels) and 4 carbon ions C^{j+}-C^{k+}-C^{m+}-C^{n+} for 1,3-butadiene (5 channels). The channels are defined as $(m, n) = (1, 1), (1,2), (2,2), (1,3), (2,3), (3,3)$; and $(j, k, m, n) = (1, 1, 1, 1), (1,1,1,2), (1,1,2,2), (1,2,2,2), (2,2,2,2)$, and are mapped in this sequence onto the 6 colors red, blue, orange, green, dark red, and dark blue. Inset in (a) for ethylene: Proton energy spectra of all 4 protons for the channel C^+-C^+.

by fragmentation along a particular channel and the black line represents the sum of all these channels. It needs to be compared to the proton spectrum without channel selection taken from Fig. 1 shown by the gray line. Because all the ejected protons of a certain channel exhibit almost identical energy spectra we only show the spectrum of one of the protons. The spectra have been normalized to 1 to allow for a direct comparison. For the higher intensity case of 1,3-butadiene we cannot decompose the proton energies $\gtrsim 35$ eV into separate channels since for $I \gtrsim 8 \times 10^{14}$ W/cm^2 the creation of the most energetic protons along fragmentation channels composed of carbon ions with a charge state higher than 2 becomes increasingly important. These channels are beyond our coincidence selection capabilities.

Knowledge of the specific fragmentation channels allows us to infer the charge state Z of the parent molecular ion before the fragmentation by simply summing up the charges of the observed protons and carbon ions for a given fragmentation channel, i.e. $Z_{mn} = 4 + m + n$ for ethylene, and $Z_{jkmn} = 6 + j + k + m + n$ for 1,3-butadiene. In order to state a certain charge for the parent molecular ion it is necessary to average over all the contributions from the various channels. To this end we define an average charge state $Z^* = \sum_i Z_i N_i / \sum_i N_i$, with Z_i the charge of channel i and N_i the number of coincidence events that contribute to this channel, i.e., the area of the proton spectrum for channel i in Fig. 2. We plot Z^* for ethylene and 1,3-butadiene in Figs. 3(a) and 3(b), respectively, as a function

of intensity. Note, that the average charge state of the parent ion thus defined is always lower than the maximum charge state that the molecule can reach with a certain probability at a given laser intensity. Therefore, in Fig. 3 we also plot the maximum observed charge state Z_i, when the channel i contributes at least with 5% to all the channels that make up the high-energy proton spectra. Note that for 1,3-butadiene Z^* and Z_i are systematically underestimated for intensities $I \gtrsim 8 \times 10^{14}$ W/cm^2.

We now turn to discuss the dynamics that leads to the high charge states and thus to the high proton energies. Ionization to such high charge states necessitates that the molecules absorb a very large amount of energy from the ionizing field. The ionization potential of an atom or molecule strongly increases with every ionization step and quickly exceeds many tens or even hundreds of eV. A scenario where the protons are ejected in a strictly sequential manner would overcome this limitation, since the charge state is lowered by 1 with every ejected proton, thereby keeping the ionization potential low throughout the pulse. However, the high proton energies cannot be explained by such a dynamics. We can also dismiss dynamic hole localization at a small distance to the proton at the time of ejection [16], since in order that all protons reach similarly high kinetic energies the hole(s) would have to accumulate always in the vicinity of the proton that is to be ejected, which appears implausible.

A likely explanation for the observed high charge states shown in Fig. 3 would be, that the molecular fragment ions are further ionized after decomposition. Then the summed up charge state of a certain fragmentation channel, Z_i, would be higher than the actual one which the proton is ejected from. We can dismiss this possibility, usually dubbed post-dissociation ionization, by simply
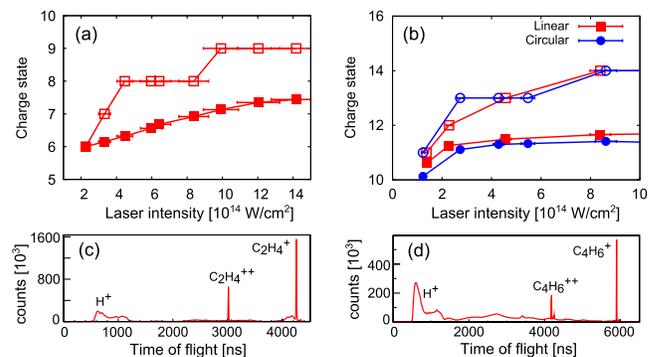

FIG. 3 (color online). (a), (b) Mean charge state Z^* as defined in the text (filled symbols) and the maximum observed charge state from all fragmentation channels, when this channel contributes at least with 5% to the overall proton spectrum (open symbols) of ethylene (a) and 1,3-butadiene (b) over laser peak intensity for linearly (squares) and circularly (circles) polarized pulses. (c),(d) Time-of-flight spectra summed over all hits per laser shot for ethylene at 4.5 (c) and 1,3-butadiene at 4.6 (d) $\times 10^{14}$ W/cm^2, respectively. The structures corresponding to the energetic protons are marked by H$^+$.

acknowledging the fact that for any two channels with charge states Z_i and Z_{i+1} we measure a higher proton energy for the higher charge state; see Fig. 2.

A way to enhance ionization and to impart energy to the molecule is electron recollision. Recolliding electrons can multiply ionize the parent ion by impact ionization, but can also impart energy to it and thus bring the ion into an excited state from which it field ionizes more easily [23]. We have repeated our experiments for 1,3-butadiene and hexane, for which the highest proton energies were observed, with circularly polarized light where no recollisions are possible. The resulting proton energy cutoffs and the reconstructed average charge states Z^* are not lower than the ones obtained for linearly polarized light; cf. blue lines in Figs. 1(g), 1(h), and 3(b). Hence, electron recollision cannot be held responsible for the high charge states.

We have shown above that all protons are ejected with consistently similar energies. Thus, they need to be ejected from the same molecular ion with charge state Z_i in a concerted Coulomb explosion with no noticeable delay between any of the individual ejections. A possible scenario that is in agreement with this and all the other observations could be the following: During the first field ionization stages at the leading edge of the pulse, the C-H bonds start to stretch until they reach the critical internuclear distance for EI [4,17,18], upon which the molecule becomes ionized several times in parallel at many different C-H bonds within a short period. Subsequently, all of the protons are removed from the highly charged ionic complex by Coulomb explosions in a concerted multiparticle fragmentation. Thereafter, the remaining structure decomposes into bare atomic carbon ions.

This scenario can also explain the thus far uncommented saturation of the measured proton energy cutoff at high intensities that we show in the insets of Figs. 1(g) and 1(h) and that also has been reported for anthracene [16]: At some threshold charge state of the parent molecule, Coulomb repulsion becomes strong enough, such that the time for the lightweight protons to depart becomes too short to permit further ionization. For increasing intensity this charge state is simply reached earlier during the pulse, but does not lead to higher proton energies. Within the proposed multibond EI scenario we can also understand why higher charge states are reached for 1,3-butadiene than for ethylene, as can be seen in Fig. 3. This is because for larger molecules EI takes place at more bonds. The increasing proton energy cutoff with increasing size of the four molecules studied, cf. Fig. 1, is thus in accordance with ejection from a higher charge state.

In Figs. 3(c) and 3(d) we show time-of-flight spectra of ethylene and 1,3-butadiene. The prominent structure corresponding to the energetic protons is marked by H^+. By comparison of the area of the structure to the rest of the spectrum it becomes obvious that the here described

fragmentation dynamics are not an exotic process but rather one of the dominant fragmentation mechanisms.

In conclusion, we demonstrated for a series of polyatomic hydrocarbon molecules a thus far unreported, yet very probable, ionization-fragmentation mechanism. We believe that the described fragmentation scenario takes place in any molecule for which the time-scale of the intramolecular nuclear motion matches the laser pulse duration. Therefore, the identified mechanism has implications for any strong-field experiment on molecules, including high harmonic generation experiments [24].

---

*markus.kitzler@tuwien.ac.at
[1] L. Frasinski *et al.*, Phys. Rev. Lett. **58**, 2424 (1987).
[2] D. Strickland *et al.*, Phys. Rev. Lett. **68**, 2755 (1992).
[3] C. Cornaggia, D. Normand, and J. Morellec, J. Phys. B **25**, L415 (1992).
[4] M. Schmidt, D. Normand, and C. Cornaggia, Phys. Rev. A **50**, 5037 (1994).
[5] C. Cornaggia, M. Schmidt, and D. Normand, Phys. Rev. A **51**, 1431 (1995).
[6] P. Hering and C. Cornaggia, Phys. Rev. A **59**, 2836 (1999).
[7] S. Shimizu *et al.*, Chem. Phys. Lett. **317**, 609 (2000).
[8] P. Hering and C. Cornaggia, Phys. Rev. A **57**, 4572 (1998).
[9] S. Palaniyappan *et al.*, Phys. Rev. Lett. **100**, 183001 (2008).
[10] M. Lezius *et al.*, J. Chem. Phys. **117**, 1575 (2002).
[11] F. Remacle and R. D. Levine, Proc. Natl. Acad. Sci. U.S.A. **103**, 6793 (2006).
[12] J. Breidbach and L. S. Cederbaum, Phys. Rev. Lett. **94**, 033901 (2005).
[13] A. Hishikawa, H. Hasegawa, and K. Yamanouchi, J. Electron Spectrosc. Relat. Phenom. **141**, 195 (2004).
[14] R. Itakura *et al.*, J. Chem. Phys. **127**, 104306 (2007).
[15] A. Hishikawa *et al.*, Phys. Rev. Lett. **99**, 258302 (2007).
[16] A. Markevitch *et al.*, Phys. Rev. Lett. **92**, 063001 (2004).
[17] T. Seideman, M. Y. Ivanov, and P. B. Corkum, Phys. Rev. Lett. **75**, 2819 (1995).
[18] T. Zuo and A. D. Bandrauk, Phys. Rev. A **52**, R2511 (1995).
[19] H. Hasegawa, A. Hishikawa, and K. Yamanouchi, Chem. Phys. Lett. **349**, 57 (2001).
[20] R. Dörner *et al.*, Phys. Rep. **330**, 95 (2000).
[21] H. Pauly, *Atom, Molecule, and Cluster Beams 1* (Springer, Berlin, 2000).
[22] A. Alnaser *et al.*, Phys. Rev. A **70**, 23413 (2004).
[23] A. Rudenko *et al.*, Phys. Rev. Lett. **93**, 253001 (2004).
[24] R. Torres *et al.*, Phys. Rev. Lett. **98**, 203007 (2007).